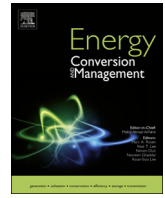




Contents lists available at ScienceDirect

Energy Conversion and Management

journal homepage: www.elsevier.com/locate/enconman

Methodology to simulate normalized testing cycles for engines and vehicles via design of experiments with low number of runs

Eloísa Torres-Jiménez^{a,*}, Octavio Armas^b, Luka Lešnik^c, Fernando Cruz-Peragón^a

^a Dep. Mechanical and Mining Engineering, University of Jaen, Campus las Lagunillas, s/n, 23071 Jaen, Spain

^b Universidad de Castilla La Mancha, Escuela de Ingeniería Industrial, Real Fábrica de Armas, Edif. Sabatini, Av. Carlos III, s/n, 45071 Toledo, Spain

^c University of Maribor, Faculty of Mechanical Engineering, Smetanova 17, SI-2000 Maribor, Slovenia

ARTICLE INFO

Keywords:

DoE
Engine performance prediction
Vehicle driving cycle
Working region mapping
Modeling
New testing methodology

ABSTRACT

This paper proposes a methodology for simulating engine/vehicle responses of a non-stationary test cycle by means of few steady-state operating modes, which can greatly reduce testing costs and time. The novelty of the proposed methodology is the application of a mapping from the engine working region to a square domain, which allows testing any design of experiments (DoE) regardless of the testing cycle, vehicle or engine. In this new working space (mapped region) it is easy to apply a DoE that satisfies optimality conditions. The validation of the methodology is based on experimental data obtained from the New European Driving Cycle. Firstly, the methodology consists in determining which representative responses can be instantaneously and/or cumulatively approximated via a low degree polynomial function (smooth surfaces) and, secondly, in performing a DoE analysis in the mapped working region where the points defining each DoE are placed. An approach function for each response is developed based on DoE tested points. Subsequently, this model allows simulating vehicle responses during the transient test. For the studied validation case, results show that main engine performance responses can be instantaneously and cumulatively predicted with high accuracy by means of a DoE with few runs. On the other hand, this analysis reveals a cumulative predicted response of confidence for regulated exhaust emissions, but not for the instantaneous values. These findings support future studies to determine the optimal DoE which minimizes testing time and costs with a satisfactory and accurate estimation of engine responses.

1. Introduction

Increasingly restrictive regulations on pollution imposed by the governments encourage researchers to optimize engine/vehicle performance and emissions. Nowadays in order to reach this target, attention is mainly focused on testing alternative fuels and decreasing fuel consumption. This kind of studies are usually based on experimental tests that follow a standardized procedure, such as the New European Driving Cycle (NEDC), which measures pollutant emissions against European Union regulations. For example, regarding alternative fuels tested under the NEDC, it is worth mention the hydrogen due to its combustion characteristics and to its no carbon-based emissions [1]. Moreover, alcohols such as ethanol and butanol lead to some environmental gains [2]. In relation to decreasing fuel consumption, several techniques are being studied such as the waste heat recovery during the NEDC [3]. New strategies over NEDC are tested in order to comply with more stringent emissions standards, such as homogenous charge

compression ignition, which shows remarkable reduction in fuel consumption and nitrogen oxides (NO_x) emissions [4]. Even more, researches have demonstrated that smart cooling control systems reduce most exhaust emissions although NO_x emissions increase, as this technique allows a better regulation of the combustion process [5].

Note that the European Union will soon switch to the new world light duty vehicle test procedure (WLTP), which is more similar to the United States cycle (the Federal Test Procedure) [6]. This is the reason why recent studies deal with the determination of the differences in exhaust emissions between the NEDC and the WLTP [7,8]. The WLTP exhibits higher pollutant emissions (NO_x and soot) compared to those of the NEDC, which is a consequence of the transient profile of the WLTP that captures much wider real-world driving representativeness than the NEDC [9–11].

In any case, emissions vary significantly in dependence on the employed engine, used fuel, and engine-operating regime, among others [12]. For this reason, experimental tests are always necessary in order

* Corresponding author.

E-mail address: etorres@ujaen.es (E. Torres-Jiménez).

<https://doi.org/10.1016/j.enconman.2018.08.061>

Received 16 May 2018; Received in revised form 15 August 2018; Accepted 16 August 2018

0196-8904/ © 2018 Elsevier Ltd. All rights reserved.

Nomenclature

CO	carbon monoxide (ppm)
CO_2	carbon dioxide emissions (%)
D matrix	design matrix
E	known input variable but uncontrollable
EGR ratio	instantaneous EGR valve position (%)
\dot{E}_{eg}	exhaust gas thermomechanical exergy rate (kW)
h_{eg}	exhaust gas specific enthalpy (kJ/kg)
h_0	exhaust gas specific enthalpy at T_0 and P_0 (kJ/kg)
k	number of measured responses
l	number of binomial coefficients in Eq. (3)
M	effective torque (Nm)
M_j	mapped effective torque
\dot{m}_a	air mass flow rate (kg/s)
\dot{m}_c	fuel mass flow rate (kg/s)
\dot{m}_{eg}	exhaust gas mass flow rate (kg/s)
n	engine speed (rpm)
n_i	mapped engine speed
NO_x	nitrogen oxides emissions (ppm)
OP	instantaneous smoke opacity (%)
P_{in}	intake manifold pressure (bar)
P_{out}	exhaust manifold pressure (bar)
P_{rail}	fuel rail pressure (bar)
P_0	ambient pressure (bar)
\dot{Q}_{eg}	exhaust gas residual heat rate (kW)
r	number of runs (number of points defining a DoE): number experiments defined by a combination of M and n
R^2 -A	R^2 considering only the points from which the approach function is generated (validation)
R^2 -B	R^2 considering the whole cycle (simulation)
R^2	coefficient of determination
s_{eg}	exhaust gas specific entropy (kJ/kg K)
s_0	exhaust gas specific entropy at T_0 and P_0 (kJ/kg K)
T_c	engine coolant temperature ($^{\circ}C$)
T_{eg}	exhaust gas temperature ($^{\circ}C$)
T_0	ambient temperature (K)

V	vehicle speed (m/s)
VFC	volumetric fuel consumption (L/s)
THC	total hydrocarbons (ppm)
x_{ij}	a combination of the factors (n, M) in Eq. (3)
y	response: output variable
y_s'	measured engine response
y_s	approximated engine response
z	factor: controllable input variable

Greek symbols

α	accelerator position (%)
β_j	polynomial coefficients of Eq. (3)
$\Delta\tau_{inj}$	main injection pulse duration (μs)
$\Delta\tau_{pre}$	pre-injection pulse duration (μs)
γ	noise: unknown and uncontrollable input variables
δ	cumulative error (%)
ε	approximation error
θ_{mit}	main injection timing (degree)
τ	test time (s)
τ_{inj}	main injection pulse timing (μs)
τ_{pre}	pre-injection pulse timing (μs)
ϕ	fuel-air equivalence ratio (-)

Abbreviations

DoE	design of experiments
ANN	artificial neural network
ECU	electronic control unit
EGR	exhaust gas recirculation
HC	hydrocarbon
NEDC	new European driving cycle
PM	particulate matter
PN	particle number
RSM	response surface methodology
TDC	top dead center
WLTP	world light duty vehicle test procedure

to optimize engine performance and emissions.

Since September 2014, Euro 6 [13] establishes the emissions limits for Diesel and Gasoline engines in Europe. In case of Diesel engines, Euro 6 limits the following emissions: carbon monoxide (CO), Hydrocarbons (HC), NO_x , particulate matter (PM), and particle number (PN). The present paper is focused on regulated emissions, leaving non-regulated emissions for a future study.

Engine performance and emissions experimental tests can be carried out in three different ways: (a) testing the whole vehicle in a rolling test bench working under the transient test, (b) testing the engine in a test bench working under the transient operating conditions obtained from the vehicle transient test via application of vehicle longitudinal dynamic equations [14,15] and (c) testing the engine in a test bench under some steady-state operating conditions belonging to the engine working region, which represent the analyzed transient test [16,17].

Normalized testing cycles are usually non-stationary tests. Determining a set of steady-state operating conditions that reproduces a non-stationary test with high accuracy has several advantages. For example, a stationary test bench is easier to monitor than a complex transient test bench. Moreover, testing few steady-state operating conditions reduces testing costs and time compared to testing the whole transient cycle. For the case of a gasoline car, previous authors have already tested the idea of simulating engine emissions of a transient test using stationary state operating conditions, with good results [18]. On the other hand, Liu et al. [19] have revealed large differences in various performance parameters of a turbocharged gasoline engine under the

NEDC in comparison with steady-state conditions. García et al. [20] and Belgiorno et al. [21] have already tested the NEDC from some operating conditions which are representative of this transient test.

Summarizing, experimental procedures, which are highly expensive and time consuming, are usually necessary to improve engine performance and emissions. These tests are usually based on the analysis of a standardized testing cycle. In the present paper, a methodology is proposed to determine if a design of experiments (DoE) with few runs (steady-state operating modes) allows reproducing a whole transient test cycle, which would allow reducing testing costs and time. These runs are defined by M (effective torque) and n (engine speed) within the engine working area derived from the standardized transient test. The key idea of the proposed methodology is to be able to apply each DoE regardless of the testing cycle, vehicle or engine. This target is reached by means of a mapping of the actual engine working region into the domain $\in [-1, 1]$. Experimental results enable modelling engine responses such as emissions, fuel consumption, and exhaust gas thermomechanical exergy rate. Once the model for each response is defined, the standardized transient test can be simulated and the cumulative responses values estimated.

In order to validate this methodology, experimental tests are carried out according to NEDC specifications in a fully equipped test bench to obtain engine performance and emissions of a common-rail diesel engine running with conventional diesel fuel. Once the experimental data are obtained, instantaneous and cumulative engine responses that can be approximated by means of smooth surfaces (they fit to a low degree

polynomial function) are identified. For these responses, the second part of this work presents a study of several DoEs with few runs. Additionally, this study is also applied to evaluate those responses with complex shapes fitted by a low degree polynomial function that provides a low cumulative error, as the cumulative response will be of confidence. All algorithms developed in the present work have been generated via Matlab® software.

The proposed methodology allows performing a “first” calibration (engine tuning) without the need to test it under a normalized transient cycle. After these results, manufacturer mounts the engine on the car, test the vehicle under that normalized transient test, and refine the engine calibration obtained from steady-state tests.

The results of this work can be taken into account as the reference for future studies regarding the determination of the optimal DoE which minimizes testing time and cost with a satisfactory accuracy.

2. Materials and methods

2.1. Experimental set-up

Main specifications of the tested engine are given in Table 1. Fig. 1 shows a scheme of the experimental set-up for steady-state and transient measurements. This engine is conforming to the European standard Euro 3. The test bench consists on an asynchronous machine model Schenck Dynas3 LI 250. The brake control system allows measuring n , accelerator position (α) and M . A specific dyno Proportional-Integral-Derivative controller setup (α/n , M/n and α/n) was adjusted in order to adapt its performance to dynamic test. The test bench is fully equipped in order to control the engine and determine most of engine operating parameters. Table 2 gives main parameters obtained through the data acquisition systems of the test bench.

Engine performance and regulated gaseous emissions derived from diesel fuel of the engine under study during NEDC were presented and analyzed in a previous work [14].

The NEDC test is a European driving cycle for assessing CO₂ emissions, pollutant emissions and fuel economy of light duty vehicles, excluding light trucks and commercial vehicles. The methodology to translate NEDC vehicle speed (V)/engaged gear versus time profile into engine speed/torque versus time profile, which was input to engine test bench, is based on vehicle longitudinal dynamic equations [14,15]. In the present work, instantaneous M and n tested in the engine are derived from the application of vehicle longitudinal dynamic equations to a Nissan Almera Tino, which is the vehicle in which the tested engine was mounted.

Additionally, exhaust gas residual heat rate (\dot{Q}_{eg}) and its thermo-mechanical exergy rate (\dot{E}_{eg}) is calculated according to Eqs. (1) and (2) respectively [22]:

$$\dot{Q}_{eg} = \dot{m}_{eg}(h_{eg}-h_0), \quad (1)$$

$$\dot{E}_{eg} = \dot{m}_{eg}[h_{eg}-h_0-T_0(s_{eg}-s_0)], \quad (2)$$

where \dot{m}_{eg} is the exhaust gas mass flow rate ($\dot{m}_{eg} = \dot{m}_a + \dot{m}_c$, where \dot{m}_a is the intake air mass flow rate and \dot{m}_c is the fuel mass flow rate), h_{eg} is the exhaust gas specific enthalpy, h_0 is the exhaust gas specific enthalpy at ambient temperature, s_{eg} is the gas specific entropy, s_0 is the exhaust gas specific entropy at ambient conditions, and T_0 is the ambient temperature.

2.2. Tested fuel

In the present study, experimental engine characteristics obtained in the test-bench described in Section 2.1 are analyzed for neat diesel fuel without additives, which is conforming to the European standard EN 590. Fuel properties were tested at Repsol Technology Centre laboratories. Main fuel properties are summarized in Table 3.

2.3. Normalized testing cycles: Conventional and proposed testing/modelling procedure

In the present section, the conventional testing and modelling procedures are briefly summarized showing the usual ways of testing, which can be performed in a rolling test bench or in a stationary test bench equipped with an asynchronous machine as a brake, and the subsequent modelling process. Next, the proposed methodology is presented to show an alternative way that allows reducing testing costs and time by means of decreasing the number of tested operating conditions.

2.3.1. Conventional procedure

Standardized tests specify vehicle speed versus time (Fig. 2: step 1.1). Example of the conventional procedure applied to a particular standardized test cycle: the NEDC). In the first conventional testing procedure (Fig. 2: procedure 1), which allows obtaining engine responses (y_s') with $s = 1 \dots k$, where k indicates the number of measured responses (e.g.: $y_1' = \alpha$, $y_2' = VFC$, $y_3' = \dot{m}_a, \dots, y_k'$) (Fig. 2: step 3), each vehicle speed corresponds to a certain value of resistance on a roller test bench (Fig. 2: step 1.2). In the second conventional procedure (Fig. 2: procedure 2), instead of testing a complete vehicle in a roller test bench, only the engine (Fig. 2: step 2.3) is tested under those operating conditions derived from the application of longitudinal dynamic equations [14,15] to the vehicle in which the engine was mounted (Fig. 2: step 2.1). This model establishes the input variables (torque and engine speed) against time (Fig. 2: step 2.2).

Once the experiment is performed, the modelling procedure consist of obtaining an approximation to engine responses via mathematical functions (Fig. 2: M.3). These approximations model engine behavior in its working area, so the modelling procedure starts with a 2D representation of torque versus engine speed by removing time from engine speed/torque versus time profiles (Fig. 2: M.1). Torque and engine speed are considered as “controllable input variables”, also called factors, (see Section 2.6). Then, a parametric equation $y_s(M,n)$ approximates each measured response $y_s'(M,n)$. The discrepancy between the exact value y_s' and the approximation to it y_s is called approximation error (ϵ) (Fig. 2: M2). From this equation, a graphic representation of each estimated response (as a function of M and n) can be obtained (Fig. 2: M3).

Nowadays, that kind of approximations are used in the calibration process of Electronic Control Units (ECU) of internal combustion engines, with the target of minimizing exhaust gas emissions and maximizing performance parameters [17]. Nevertheless, this stage of the calibration process is quite expensive and time-consuming as it needs a large number of experimental tests if a high accuracy approximation function to engine responses is required.

Table 1

Main specifications of the tested engine.

Engine manufacturer	NISSAN
Fuel injection system	Common-rail
Number of cylinders	4, in line
Air intake system	Turbocharged – Intercooled
Cycle	4 stroke
Injection pressure	250 bar at idle (750 rpm)/1600 bar at max rated power
Number and relative position of injections	1 pre-injection before TDC ^a , 1 main injection after TDC
EGR ratio	High pressure, external, hot. Max EGR ratio < 40%
Rated power condition	82 kW (at 4000 rpm)
Peak torque condition	248 Nm (at 2000 rpm)
Compression ratio	16.7:1

^a Top dead centre.

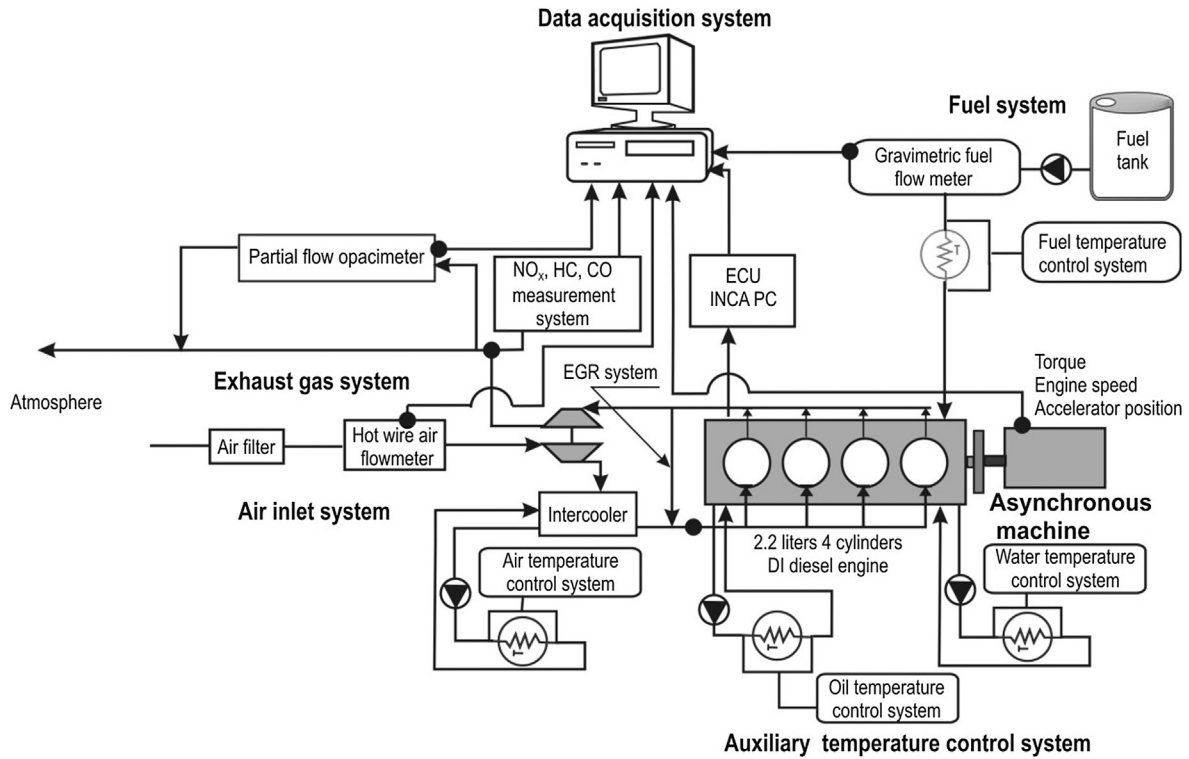


Fig. 1. Scheme of the experimental set-up.

2.3.2. Alternative procedure (proposed methodology)

The present methodology tries to obtain the same results as the conventional methodologies but decreasing time and testing costs, i.e. it tries to estimate engine responses $y_s(M,n)$ by means of few steady-state operating conditions. To reach this target, establishing a DoE within the engine working area is essential. Each run of the DoE defines a steady-state operating condition. Each response obtained, when testing these operating conditions, provides a model, which, subsequently, allows simulating the responses of the conventional transient test (see Fig. 3).

2.4. Validation of the methodology

The steps to validate the alternative procedure are as follows:

Step 1. Follow the conventional testing procedure 2 in order to obtain the approach functions of each representative engine response as a function of M and n factors (see Fig. 2: M3). In the present study, responses from the engine under study (see Section 2.1) during NEDC are analyzed.

Table 3 Diesel fuel properties.

Property	Unit	EN 590 limits min/Max	Tested fuel D100
Density at 15 °C	kg/m ³	820/845	835
Cold filter plugging point	°C	climate-dependent requirements	-18
Derived Cetane Number (IQT)	-	Cetane number min 51	54.88
Sulphur content	mg/kg	Max 10	4.96
Neat Calorific value	MJ/kg	-	42.5
Kinematic viscosity (40 °C)	mm ² /s	2/4.5	2.718
Water content	mg/kg	Max 200	57
Acid number	mg KOH/g	-	0.085

Table 2 Parameters experimentally obtained.

Test bed type: asynchronous machine model Schenck Dynas3 LI 250

Measured parameter	Symbol and unit	Measured parameter	Symbol and unit
Engine speed	n (rpm)	Engine coolant temperature	T_c (°C)
Accelerator position	α (%)	Oil temperature	T_{oil} (°C)
Effective torque	M (Nm)	Intake manifold pressure	P_{in} (bar)
Air mass flow rate	\dot{m}_a (kg/s)	Exhaust manifold pressure	P_{out} (bar)
Instantaneous EGR valve position	EGR ratio (%)	Fuel rail pressure	P_{rail} (bar)
Volumetric fuel consumption	VFC (L/s)	Main injection timing	θ_{mit} (degree)
Instantaneous smoke opacity	OP (%)	Fuel-air equivalence ratio	ϕ (-)
Nitrogen Oxides emissions	NO_x (ppm)	Pre-injection pulse timing	τ_{pre} (μ s)
Total hydrocarbons	THC (ppm)	Pre-injection pulse duration	$\Delta\tau_{pre}$ (μ s)
Carbon monoxide	CO (ppm)	Main injection pulse timing	τ_{inj} (μ s)
Carbon dioxide emissions	CO_2 (%)	Main injection pulse duration	$\Delta\tau_{inj}$ (μ s)
Exhaust gas temperature	T_{eg} (°C)		

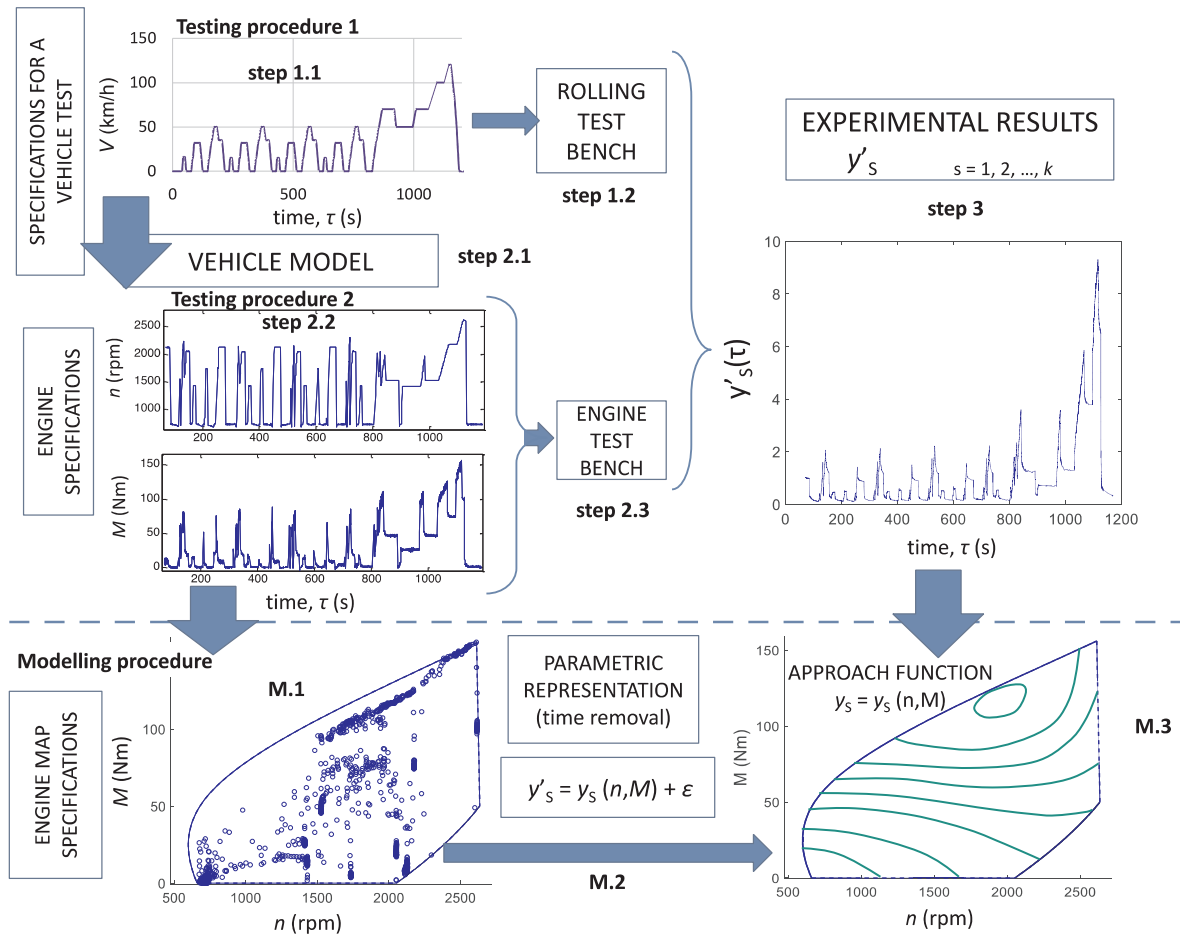


Fig. 2. Conventional testing and modelling procedures.

Step 2. Determine which representative responses can be approximated via smooth-surfaces according to the procedure described in Section 2.5. Additionally, engine responses approximated via a smooth-surface which provides a low cumulative error are analyzed. Step 3. Evaluate several DoE (see Section 2.6):

- Define a surrounding curve of the engine working area defined by M and n (see Fig. 3).
- Perform a mapping of the engine working region into the domain $\in [-1, 1]$.
- Place the points of each DoE proposed in Section 2.6 on the mapped working region.
- Test the operating conditions selected by the proposed DoE.
- Develop an approach function (model) of each selected response based on the few runs given by the tried DoE.
- Finally, the previously obtained models are used to simulate vehicle/engine responses during the transient test (in this case: the NEDC), so that they can be compared to those obtained from the conventional testing procedure. A comparison between experimental and estimated responses can be evaluated by means of the determination coefficient (R^2) and the cumulative error (δ) (see Section 3.2).
- DoEs with R^2 close to 1 reveal a successful application of the proposed methodology, as the instantaneous and cumulative responses can be predicted with high accuracy. Moreover, even with a low R^2 , if δ is very low, the methodology gives useful results, as the predicted cumulative response is reliable.

2.5. Approximation to responses

In order to obtain a simple numerical model, the resulting approximations should be smooth surfaces; otherwise, more complex equations must be developed to try to reproduce the actual response surface. In the present work, a linear regression is used to obtain an approach of each response analyzed ($y_s = f(n, M)$). The function represents a smooth surface if it corresponds to a low-degree polynomial (see Eq. (3):

$$y_s = \sum_{j=0}^{j=l} \beta_j x_{ij} \quad (3)$$

where β_j are the polynomial coefficients and x_{ij} are combinations of the selected two factors (M, n). Each couple of data (M, n) corresponds to an operating mode i (a steady-state operating condition) from a total of r runs ($i = 1 \dots r$). These combinations are selected following the Pascal's triangle [23], which defines a triangular array of the binomial coefficients of length l ($j = 1 \dots l$). For example, for $l = 9$ the resulting combinations are as follows: $x_{i0} = 1, x_{i1} = n, x_{i2} = M, x_{i3} = n^2, x_{i4} = nM, x_{i5} = M^2, x_{i6} = n^3, x_{i7} = n^2M, x_{i8} = nM^2, x_{i9} = M^3$.

According to the Response Surface Methodology (RSM) [24], for this type of surfaces, a DoE with few runs (number of testing operating conditions or combination of the two factors) can be determined, which, in short terms, is one of the keys of an optimal design [25]: in order to approximate first-degree trend surfaces, at least 4 runs are required; additionally, for second-degree trend surfaces, a minimum of 9 runs is required; finally, for third-degree trend surfaces, a minimum of 13 runs must be reached [26].

Note that the idea is to try to simulate a non-stationary test (in this

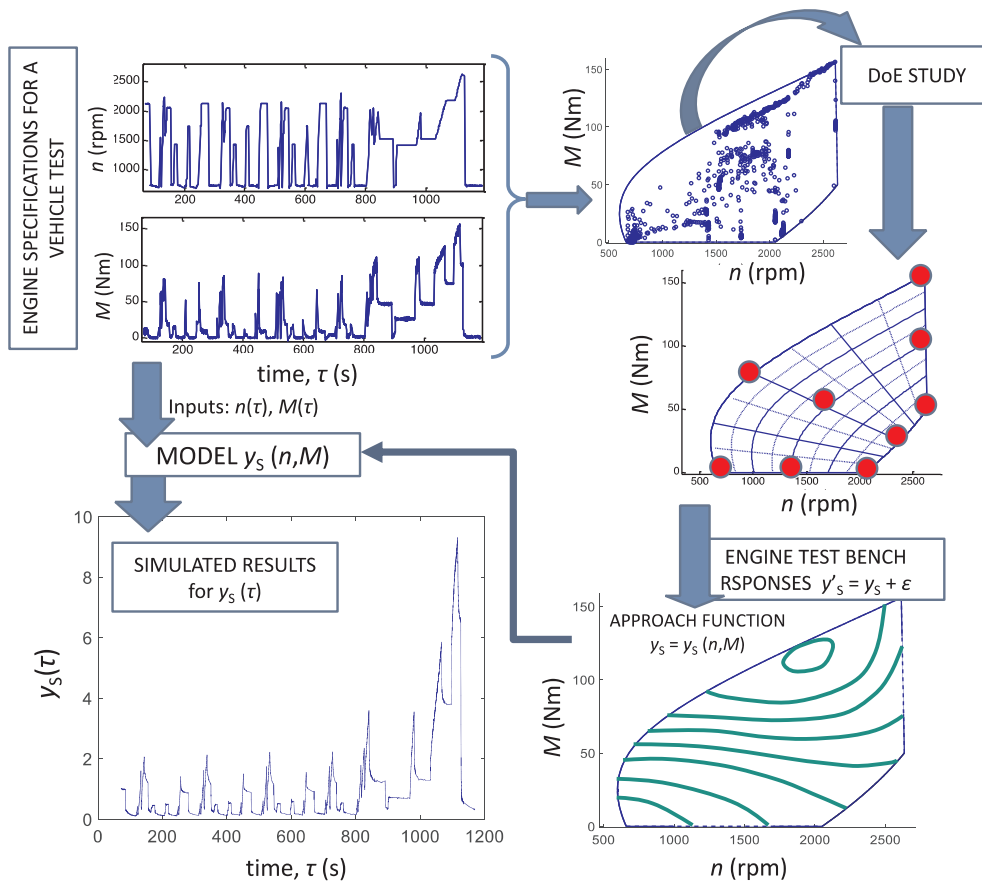


Fig. 3. NEDC: Alternative testing and modelling procedures.

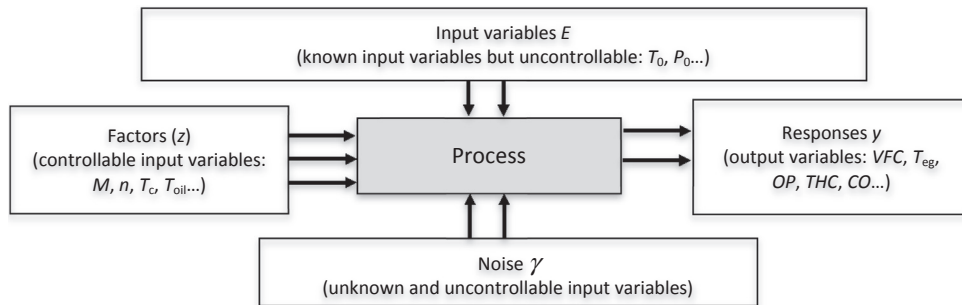


Fig. 4. DoE method: factors and responses.

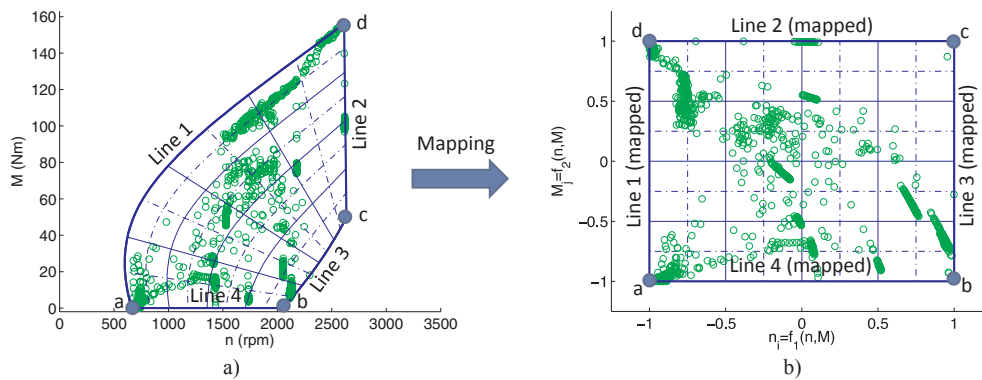


Fig. 5. (a) Torque-engine speed map from NEDC test, (b) Mapping of the torque-speed engine map in the $[-1, 1]$ domain.

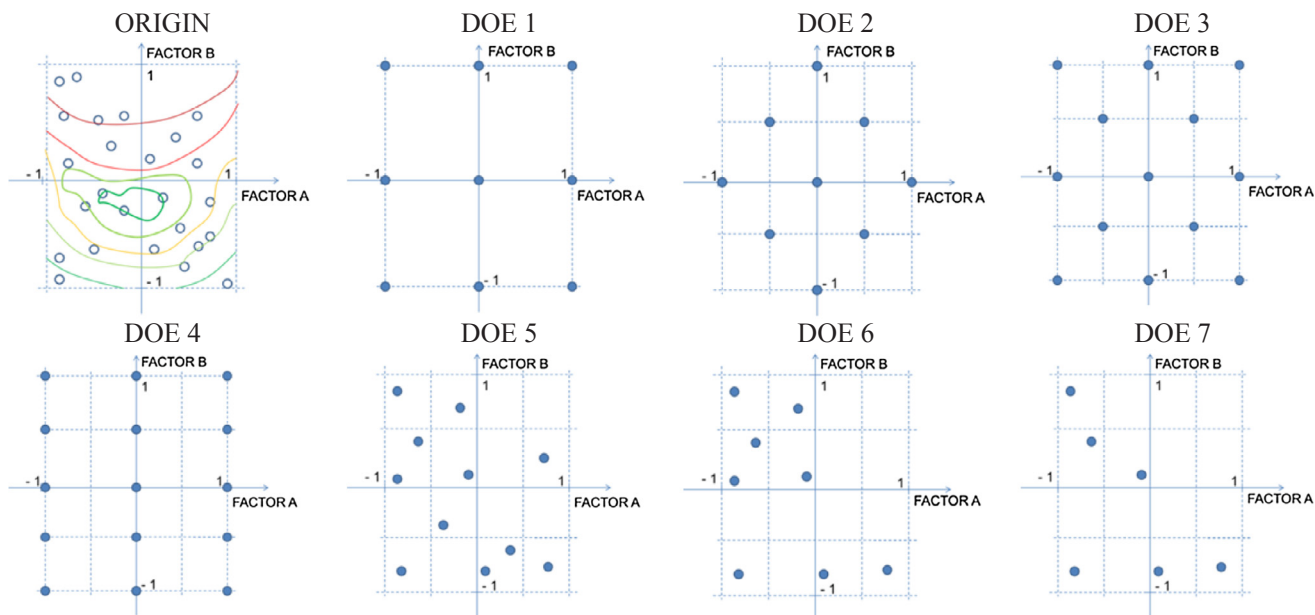


Fig. 6. Evaluated designs.

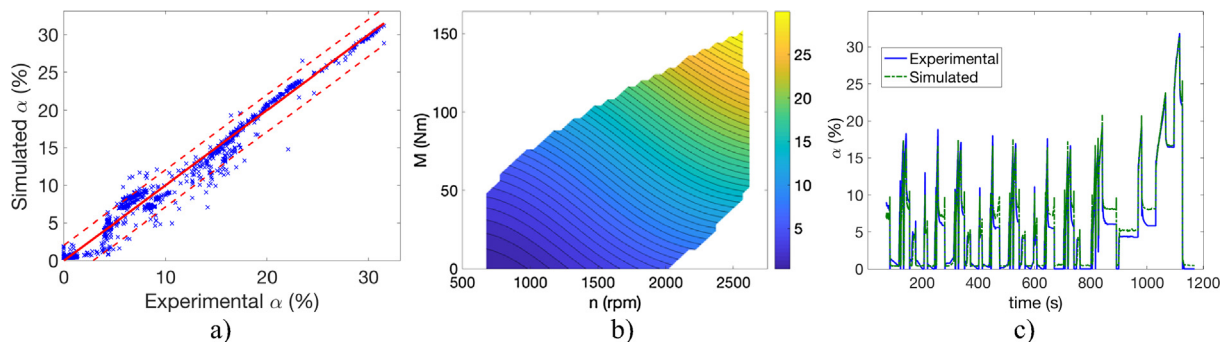
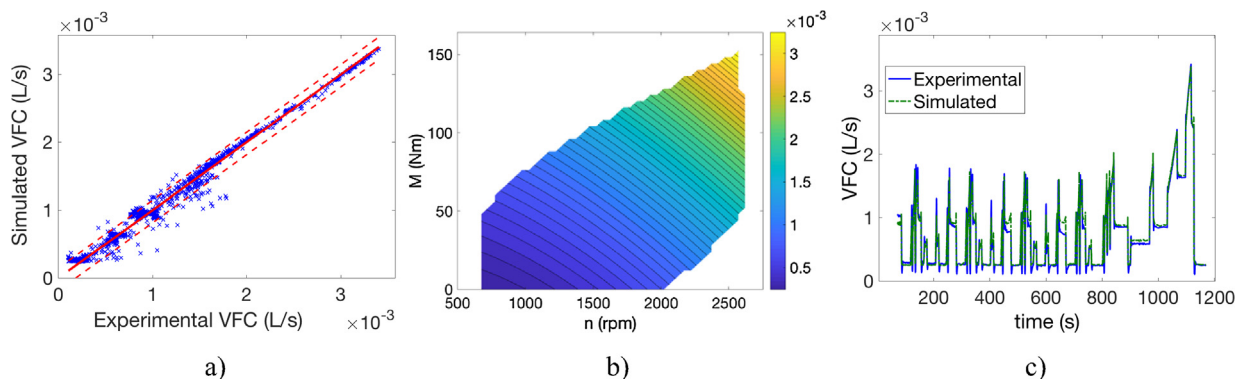
Fig. 7. α response (polynomial approximation): (a) skew plot correlation data with a confidence interval of 95%, (b) contour plot of the approximated response surface, (c) NEDC: comparison between measured and estimated response.

Fig. 8. VFC response (polynomial approximation): (a) skew plot correlation data with a confidence interval of 95%, (b) contour plot of the approximated response surface, (c) NEDC: comparison between measured and estimated response.

case: the NEDC) based on stationary operating conditions tests. If the actual experimental data form a non-smooth surface, a nonlinear function is needed, which requires increasing the number of runs, therefore, those responses are not suitable for a DoE analysis. Complex surfaces can be approximated, for example, via an artificial neural network (ANN) [27].

Summarizing, the methodology to approximate the actual surfaces built by means of experimental data obtained from a standardized

transient test is as follows:

- Select the most representative parameters of the standardized transient test (see Section 2.1).
- From the non-stationary test, select those instantaneous data in which the derivative of the accelerator position ($d\alpha/d\tau$) is very low, so that those points could represent steady-state conditions.
- Try a second or third order polynomial to approach each

Table 4
Quality of several approximations to responses. Determination coefficients R^2 -A and R^2 -B and cumulative error δ .

Response	Function type (polynomial or ANN)	R^2 -A	R^2 -B	δ (%)
α (%)	Second-order polynomial	0.9784	0.9676	–
α (%)	Third-order polynomial	0.9795	0.9678	–
α (%)	ANN (2 factors)	0.98645	0.97091	–
VFC (L/s)	Second-order polynomial	0.987	0.9256	1.67
VFC (L/s)	Third-order polynomial	0.9877	0.9175	2.2388
VFC (L/s)	ANN (2 factors)	0.9882	0.9119	2.5
\dot{m}_a (kg/s)	Second-order polynomial	0.9759	0.9754	4
\dot{m}_a (kg/s)	Third-order polynomial	0.9773	0.9728	4.4
\dot{m}_a (kg/s)	ANN (2 factors)	0.982	0.973	3.26
P_{rail} (bar)	Second-order polynomial	0.9904	0.9617	1.525
P_{rail} (bar)	Third-order polynomial	0.9916	0.9739	1.027
P_{rail} (bar)	ANN (2 factors)	0.997	0.98	0.31
\dot{Q}_{eg} (kW)	Second-order polynomial	0.9872	0.9677	1.83
\dot{Q}_{eg} (kW)	Third-order polynomial	0.9887	0.9694	1.95
\dot{Q}_{eg} (kW)	ANN (2 factors)	0.995	0.9777	3.14
\dot{E}_{eg} (kW)	Second-order polynomial	0.9777	0.9487	0.44
\dot{E}_{eg} (kW)	Third-order polynomial	0.9803	0.9532	1.03
\dot{E}_{eg} (kW)	ANN (2 factors)	0.9935	0.9657	2.69
T_{eg} (°C)	Second-order polynomial	0.722	0.592	–
T_{eg} (°C)	Third-order polynomial	0.7294	0.6083	–
T_{eg} (°C)	ANN (2 factors)	0.8607	0.7314	–
T_{eg} (°C)	ANN (multiple factors)	0.9353	0.9353	–
EGR ratio	Second-order polynomial	0.5233	0.5509	–
EGR ratio	Third-order polynomial	0.5518	0.5217	–
EGR ratio	ANN (2 factors)	0.7156	0.6325	–
EGR ratio	ANN (multiple factors)	0.9117	0.9117	–
OP (%)	Second-order polynomial	0.691	0.5404	–6.29
OP (%)	Third-order polynomial	0.74537	0.58524	–2.6
OP (%)	ANN (2 factors)	0.915	0.73011	3.2
OP (%)	ANN (multiple factors)	0.893	0.893	0.947
THC (ppm)	Second-order polynomial	0.7481	0.6603	19.6
THC (ppm)	Third-order polynomial	0.8045	0.7198	16.955
THC (ppm)	ANN (2 factors)	0.895	0.6655	20.3
THC (ppm)	ANN (multiple factors)	0.949	0.949	0.271
NO_x (ppm)	Second-order polynomial	0.90405	0.78652	10.7809
NO_x (ppm)	Third-order polynomial	0.90997	0.7868	10.05
NO_x (ppm)	ANN (2 factors)	0.93992	0.86043	4.095
NO_x (ppm)	ANN (multiple factors)	0.939	0.939	3.89
CO_2 (%)	Second-order polynomial	0.9552	0.8581	–0.4932
CO_2 (%)	Third-order polynomial	0.9605	0.8208	0.4918
CO_2 (%)	ANN (2 factors)	0.9699	0.8734	0.225
CO_2 (%)	ANN (multiple factors)	0.9279	0.9279	0.8811
CO (ppm)	Second-order polynomial	0.7470	0.5967	20.8730
CO (ppm)	Third-order polynomial	0.8034	0.6553	15.81
CO (ppm)	ANN (2 factors)	0.8682	0.6741	11.187
CO (ppm)	ANN (multiple factors)	0.8826	0.8826	0.4008
$\Delta\tau_{pre}$ (μ s)	Second-order polynomial	0.95698	0.86025	–
$\Delta\tau_{pre}$ (μ s)	Third-order polynomial	0.9595	0.82131	–
$\Delta\tau_{pre}$ (μ s)	ANN (2 factors)	0.96148	0.85309	–
$\Delta\tau_{pre}$ (μ s)	ANN (multiple factors)	0.9568	0.9568	–
$\Delta\tau_{iny}$ (μ s)	Second-order polynomial	0.8019	0.62156	–
$\Delta\tau_{iny}$ (μ s)	Third-order polynomial	0.81529	0.50616	–
$\Delta\tau_{iny}$ (μ s)	ANN (2 factors)	0.86215	0.62958	–
$\Delta\tau_{iny}$ (μ s)	ANN (multiple factors)	0.9031	0.9031	–

representative response and evaluate the goodness of fitting via the coefficient of determination R^2 and the cumulative error δ . The determination coefficient for a linear regression is the quotient of the variances of the fitted values and observed values of the dependent variable, meanwhile the cumulative error over time interval τ of the test is calculated as follows Eq. (4) [28]:

$$\delta = 100 \cdot \frac{\int_{\tau} (y'_s - y_s) d\tau}{\int_{\tau} y'_s d\tau} \quad (4)$$

- Select those responses with a high R^2 and a low δ .

Rest of parameters must be approximated in different ways, but they would not be appropriate for a DoE analysis with few runs. For example, in the present paper an ANN is used, in concordance with the works of previous authors [29–32]. This study needs a deep analysis, so we will try a basic, but effective, ANN model. This model corresponds to a multilayer Backpropagation network with two internal layers, tangent sigmoid activation function, using a Levenberg-Marquardt training algorithm [33] into a regularization method [34] in order to avoid overfitting during training. This kind of network was previously used in other fields with accurate results by the authors [35].

2.6. Proposed DoE

Design of Experiments is a method to determine the relationship between input variables affecting a process (factors) and the output of that process (responses) (see Fig. 4). Regarding input variables, E is the vector containing those variables that are known but uncontrollable (see Fig. 4), such as geometrical characteristics of the fuel injection system or environmental conditions. Additionally, taking into consideration that the noise (γ) leads to determine an external matrix, which complicates the analysis without increasing significantly the accuracy of the approximation, this influence will be neglected. Nevertheless, in order to minimize some of these possible effects, experimental tests are carried out several times and not in the same order, i.e. the planning of the testing sequence from one operating mode to the next one is random.

In this case, the target is to select a DoE with few runs, where each run fixes a steady-state operating condition defined by two factors (M , n). A decrement in testing cost and time can be reached if DoE responses can provide a model which properly reproduces engine/vehicle responses under the studied transient test cycle. Wu and Hamada [24] describe the DoE methodology and provide a wide array of designs, such as: full-factorial designs and fractional-factorial designs. The modelling technique will be based on the response surface methodology (RSM), which explains that, although in general such a relationship is unknown, it can be approximated by a low-degree polynomial model such as the Bayesian approach [25].

A specific DoE includes r points (runs), which means r experiments defined by a combination of the two factors (M , n). The combinations x_{ij} from Eq. (3) constitutes the so-called response surface design (or design), which can be represented by the following design matrix D :

$$D = \begin{bmatrix} x_{11}x_{12} \cdots x_{1l} \\ x_{21}x_{22} \cdots x_{2l} \\ \vdots \\ x_{r1}x_{r2} \cdots x_{rl} \end{bmatrix}$$

In order to place each point of a DoE in the engine-working region it is essential to perform a mapping, i.e., the workspace must be located between values $[-1,1]$ for the two control variables [24,25]. This is important for two reasons: first, this mapping generalizes the working region so that it is independent from the vehicle or engine tested, on the other hand, in this mapped region, DoE optimality conditions are easier to apply.

The test selected to apply the proposed methodology is the NEDC test. The analysis of this transient test allows evaluating a torque-speed map (Fig. 5a) and know where the engine operates during the test (circle points in Fig. 5a).

In order to reach the target of mapping the actual engine working region into a square domain, four polynomial curves (lines 1 to 4 in Fig. 5a) are drawn to define the boundary of a planar patch, which encloses the engine working region. These boundaries are mapped into the edges of a square domain, whose vertices are the four endpoints a, b, c and d in Fig. 5. For the interior of the region, a set of isoparametric curves are constructed using the working region boundaries and the square domain parameters: $n_i \in [-1, 1]$ for curves between lines 2 and 4, and $M_j \in [-1, 1]$ for curves between lines 1 and 3. Since the

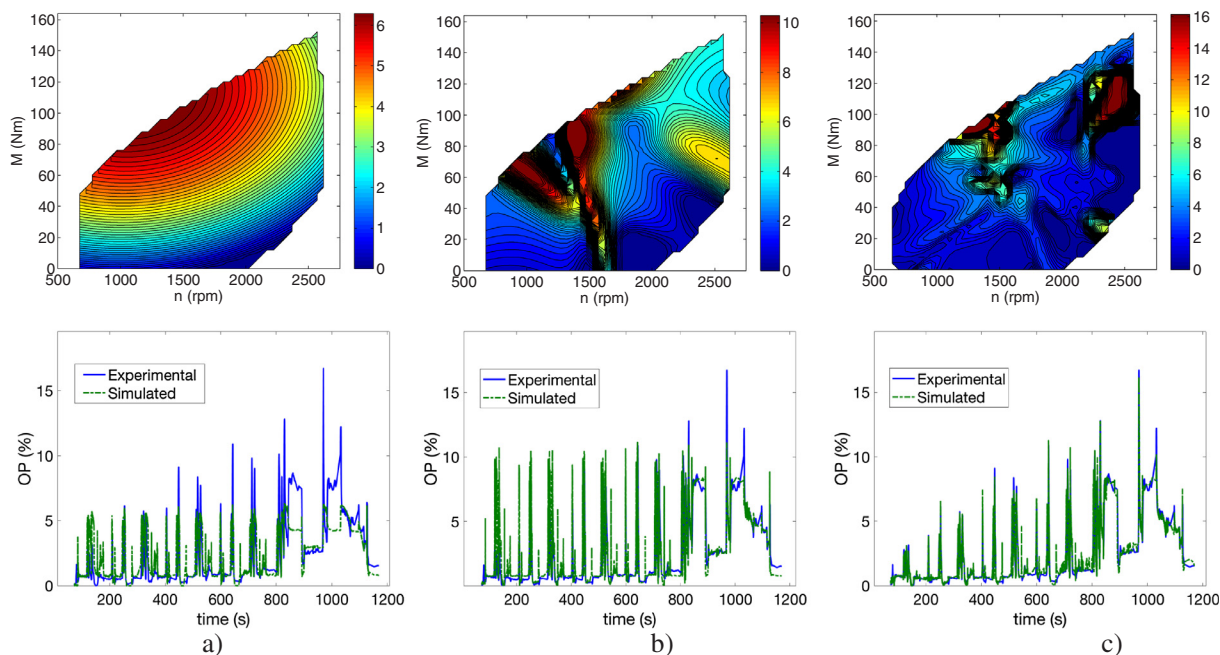


Fig. 9. Opacity response, contour plot and measured/estimated response during NEDC test: (a) polynomial approximation with 2 factors (M and n), (b) ANN approximation with two factors (M and n), (c) ANN approximation with multiple factors.

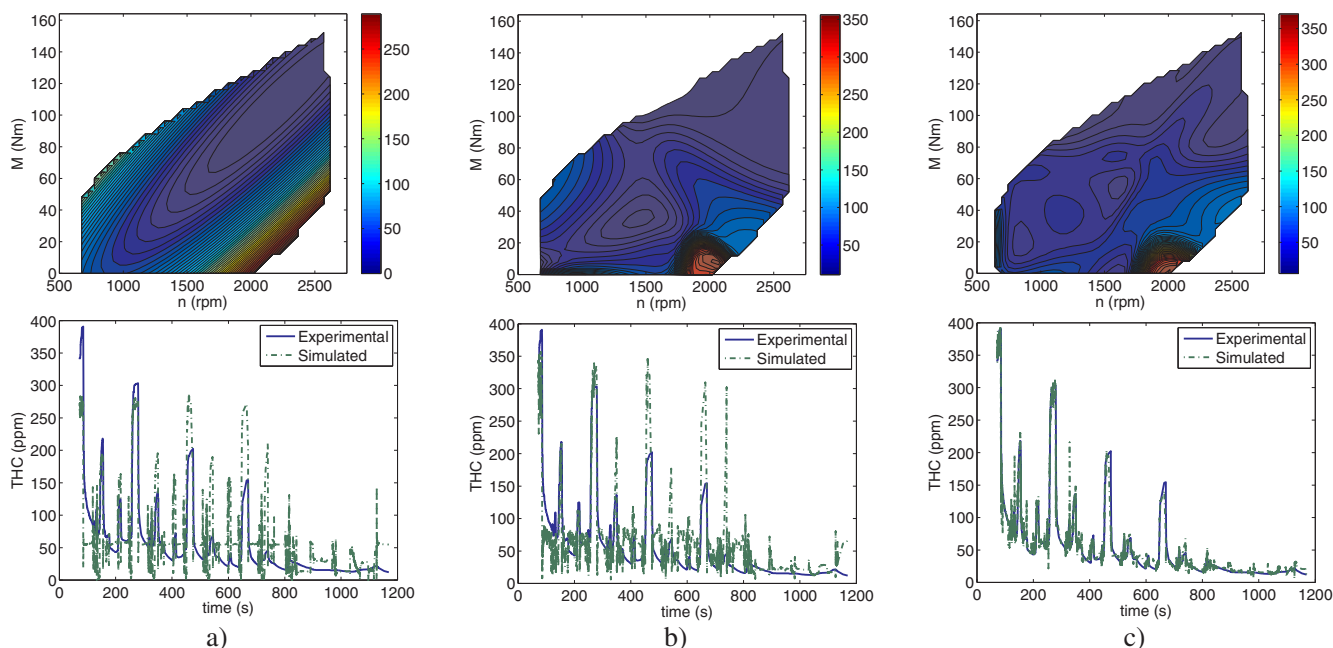


Fig. 10. THC response: contour plot and measured/estimated response during NEDC test: (a) polynomial approximation with 2 factors (M and n), (b) ANN approximation with two factors (M and n), (c) ANN approximation with multiple factors.

correspondence between isoparametric curves and square domain parameter values is known, each measured point within the working region is mapped into a point in the square domain by interpolating the isoparametric curves that enclose this point, so that: $\{n_i, M_j\} = \{f_1(n, M), f_2(n, M)\}$.

DoEs tested in this study are shown in Fig. 6. Those designs were selected for several reasons: some of them satisfy some optimality criteria and the rest of designs were proposed by Cárdenas [16] as a set of steady-state operating conditions that can represent the whole NEDC test. Consequently, these DoE could be an adequate choice just in the case that the transient test cycle under study corresponds to the NEDC.

In the new workspace, the test matrices showed in Fig. 6 are

defined:

- DOE 1. This design is a three levels full factorial design and can be denoted as “ 3^2 design”, which means three levels for each of the two factors. A second order adjustment is used in this design. This is the simplest 3-level design with only 2 factors (a 3×3 factorial design, which means 9 runs).
- DOE 2. Central composite design (9 runs), with a second order adjustment. Central composite designs are fractional factorial designs composed of center points and a group of axial points (also called star points) that allow estimating curvature.
- DOE 3. Fractional factorial design (5 levels, 13 runs). The higher

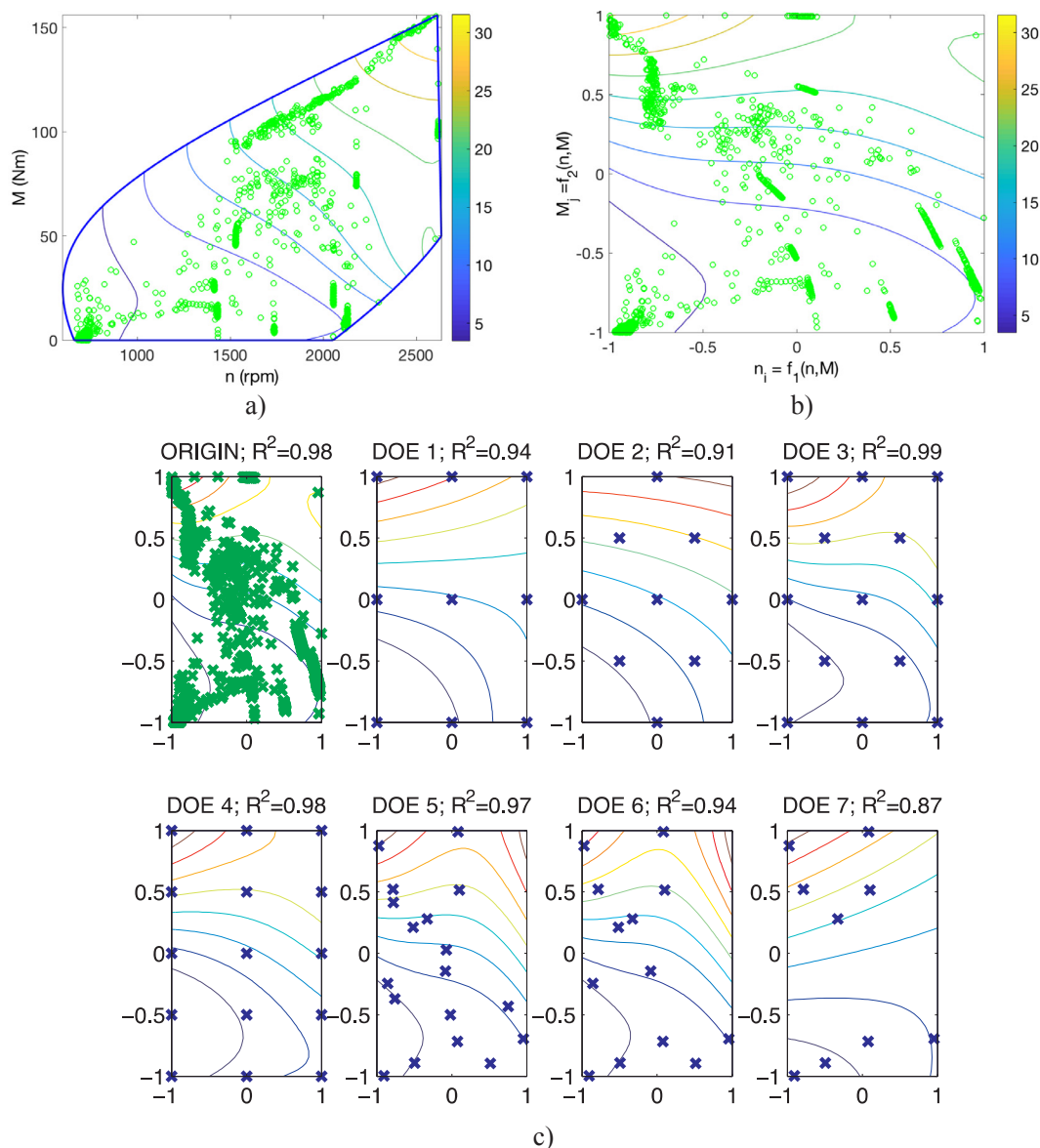


Fig. 11. Contour plots of the accelerator position response: (a) original surface in the domain n , M (actual engine working space), (b) mapping surface in the domain n_i , $M_j \in [-1, 1]$, (c) DoE data including the determination coefficient for each of the seven designs proposed.

number of runs allows a third order adjustment.

- (d) DOE 4. Full factorial design with 3 levels for the factor in X-axis and 5 levels for the factor in Y-axis. This is an orthogonal design of 15 runs, which allows a third order adjustment.
- (e) DOE 5: This design consists of 18 runs. This number of runs allows a third order adjustment. Design 5 is the reference for designs 6 and 7. These operating modes were identified in a previous study as the equivalent steady-state modes that represent each sequence of the NEDC test [16]. Taking into account characteristics of each sequence (initial and final vehicle speed, engaged gear and time) the corresponding equivalent steady-state mode can be determined according to [15]. Applying this procedure to each identified cycle sequence, Cárdenas [16] determined 18 steady-states modes which represent the NEDC.
- (f) DOE 6: This design is composed of 13 runs selected from DOE 5. Thirteen runs correspond to the minimum number of runs required to perform a third order adjustment.
- (g) DOE 7: This design is composed of 9 runs selected from design 5. Nine runs correspond to the minimum number of runs required to perform a second order adjustment.

Designs from 1 to 4 satisfy some optimality conditions (orthogonal, rotatable, of uniform precision, and have a high D -optimal value and low space filling) [25]. Designs 6 and 7 are based on design 5. The adjustment provided by DOE 5 (18 runs) is of high accuracy, as it was designed specifically to reproduce the NEDC test. DOE 6 (13 runs) and DOE 7 (9 runs) show just some runs of DOE 5 with the target of testing the suitability of decreasing, even more, the number of runs. Although designs 5, 6 and 7 could establish good approximations, they cannot be generalized to other test cycles.

In summary, different DoE designs are presented, and they will be evaluated based on the number of runs needed and the fitting agreement. Subsequently, the response surface resulting from the transient test is evaluated and compared to that obtained if only the design points are taken. This procedure will be evaluated for several responses. The results will be analyzed and, finally, some DoE with few runs will be proposed for the determination of engine responses.

3. Results and discussion

In this work, the analyzed responses $y_s'(M, n)$ are the most

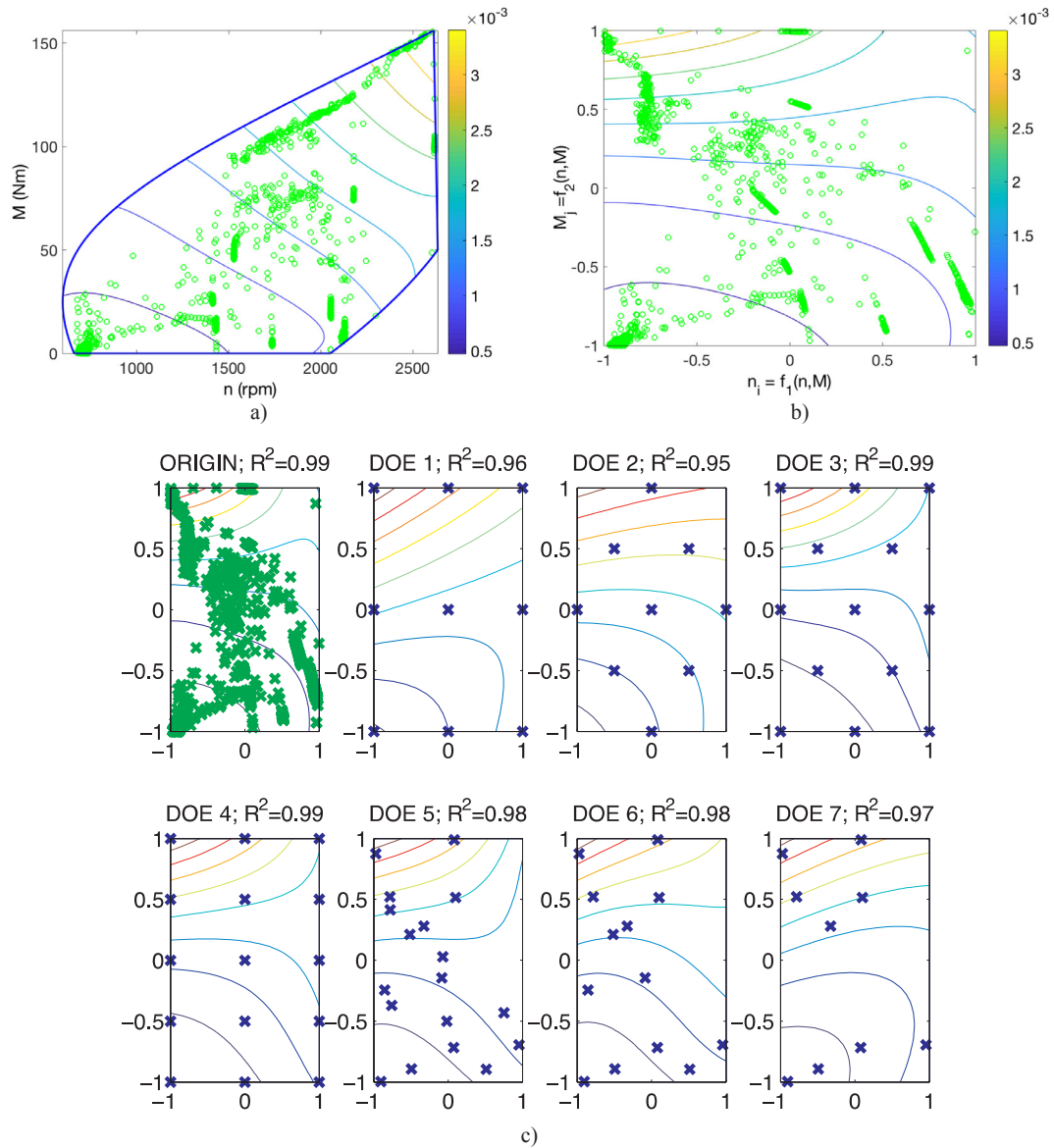


Fig. 12. Contour plots of the volumetric fuel consumption response: (a) original surface in the domain n, M (actual engine working space), (b) mapping surface in the domain $n_i, M_i \in [-1, 1]$, (c) DoE data including the determination coefficient for each of the seven designs proposed.

representative parameters of NEDC test (see Table 2). These responses are as follows: α , VFC , \dot{m}_a , P_{rail} , \dot{Q}_{eg} , \dot{E}_{eg} , T_{eg} , EGR ratio, OP , THC , NO_x emissions, CO , CO_2 , $\Delta\tau_{pre}$ and $\Delta\tau_{inj}$.

3.1. Approximation surfaces to responses

Because approximations are built only with data which derivative of accelerator position is very low, a first determination coefficient is calculated from them (R^2 -A) for validating the function. Additionally, R^2 -B is the determination coefficient obtained by comparing all the instantaneous data of the test cycle with those simulated from the approached function.

Figs. 7 and 8 show an example of smooth approximation surfaces built by means of polynomial functions (quadratic or cubic) for the following responses: accelerator position and volumetric fuel consumption, both in dependence of n - M .

Table 4 summarizes the determination coefficients (R^2 -A and R^2 -B) values obtained for each response analyzed, together with the function type applied and the cumulative error δ . In case of ANN approximation for EGR ratio and T_{eg} responses with multiple factors, all testing points

of NEDC test are taking into account, for this reason R^2 -A = R^2 -B, and those factors are: M , n , T_c , T_{oil} and accelerator position derivative. Note that, for some responses (α , T_{eg} , EGR ratio, $\Delta\tau_{pre}$, $\Delta\tau_{inj}$) it doesn't make any sense to calculate the cumulative error, since cumulative responses are representative just in some cases, such as for the case of emissions responses.

According to Table 4, responses approximated via smooth surfaces (second or third order polynomial) with enough accuracy ($R^2 > 0.9$ and $\delta \leq 5\%$) and based just on stationary data are: accelerator position, volumetric fuel consumption, air mass flow rate, rail pressure, exhaust gas residual heat rate, and exhaust gas thermomechanical exergy rate. These responses are initially selected for the DoE analysis (see Section 3.2). Additionally, none of the functions analyzed can instantaneously approximate with sufficient accuracy (not high enough R^2) all emissions responses. This is in concordance with the results obtained by previous authors, such as [36] which cannot provide a $R^2 > 0.75$ for CO and HC emissions, as well as with other works [14,37–40] where remarkable dispersion values between experimental and simulated results were obtained. Nevertheless, according to Table 4, the greater δ for a third order adjustment is 17%, which can be considered

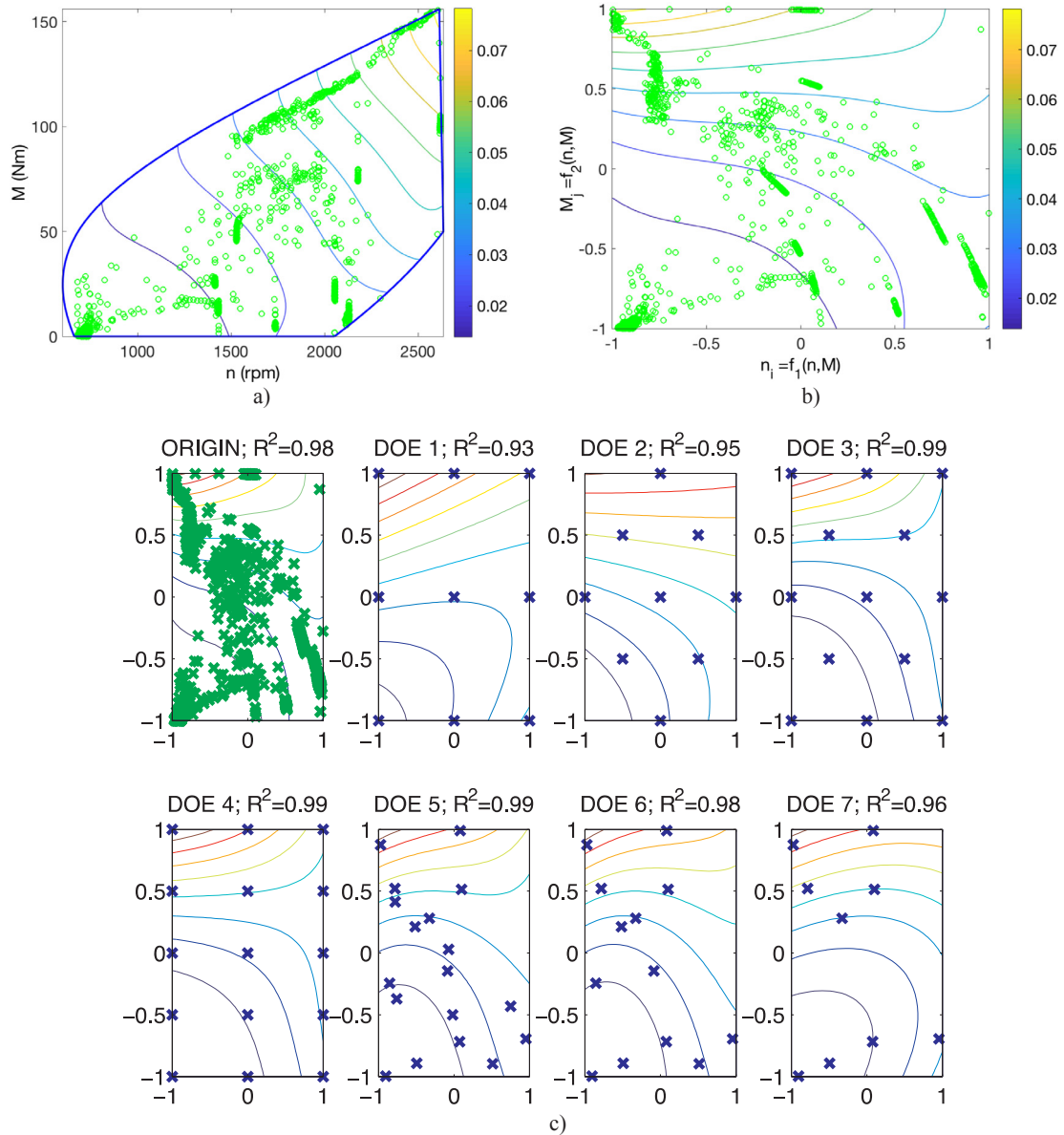


Fig. 13. Contour plots of the air mass flow rate response: (a) original surface in the domain n, M (actual engine working space), (b) mapping surface in the domain $n_i, M_j \in [-1, 1]$, (c) DoE data including the determination coefficient for each of the seven designs proposed.

satisfactory enough to provide a prediction with sufficient accuracy of cumulative responses. For this reason, and due to the importance of exhaust emissions, a DoE analysis for these responses will be included in the present paper as well.

Although smooth surfaces cannot provide a good approximation for emissions and the rest of responses with low R^2 , more complex functions, such as ANN, can do it. An ANN with only 2 input factors (M, n) and based just on stationary data does not lead to approximations with enough accuracy. Nevertheless, the following responses can be approximated by increasing the number of factors and taking into account all testing points of NEDC test, i.e. including transient conditions (for this reason $R^2\text{-A} = R^2\text{-B}$): T_{eg} , EGR ratio, OP , THC , NO_x , CO_2 , CO , $\Delta\tau_{pre}$ and $\Delta\tau_{inj}$. The exhaust gas temperature cannot be predicted with enough accuracy but, the exhaust gas residual heat rate polynomial gives a very good approximation, which in our opinion, is more important because it allows studying the potential of engine energy recovery. EGR ratio as well as the rest of injection parameters, with the exception of P_{rail} , cannot be approximated by means of smooth surfaces, so they are not appropriate for the DoE analysis. This is not a significant drawback

since these parameters could be obtained from the engine maps available in the ECU (Electronic Control Unit). For this reason, none of them will be taken into consideration in Section 3.2 and, henceforth, these parameters will be considered as “input variables” (see Fig. 4). Finally, although all responses can be approximated via an ANN, in order to obtain enough accuracy, too many factors are needed and the resulting surface has a high non-linearity, so they are not appropriate for a DoE analysis with few runs, except in the case of harmful emissions for the reasons previously mentioned.

Next, some examples of high non-linear approximation surfaces are shown. Figs. 9 and 10 portray the contour plot and the comparison between measured and estimated OP and THC emissions responses values during NEDC test. These approximations are performed through: (a) polynomial with 2 factors (M and n), (b) ANN with two factors (M and n), and (c) ANN with multiple factors ($M, n, T_c, T_{oil}, \alpha, EGR$ and T_{eg}). These figures show how the estimation improves by means of increasing the complexity of the approximation. Their coefficients of determination ($R^2\text{-A}$, $R^2\text{-B}$ and R^2) are shown in Table 4.

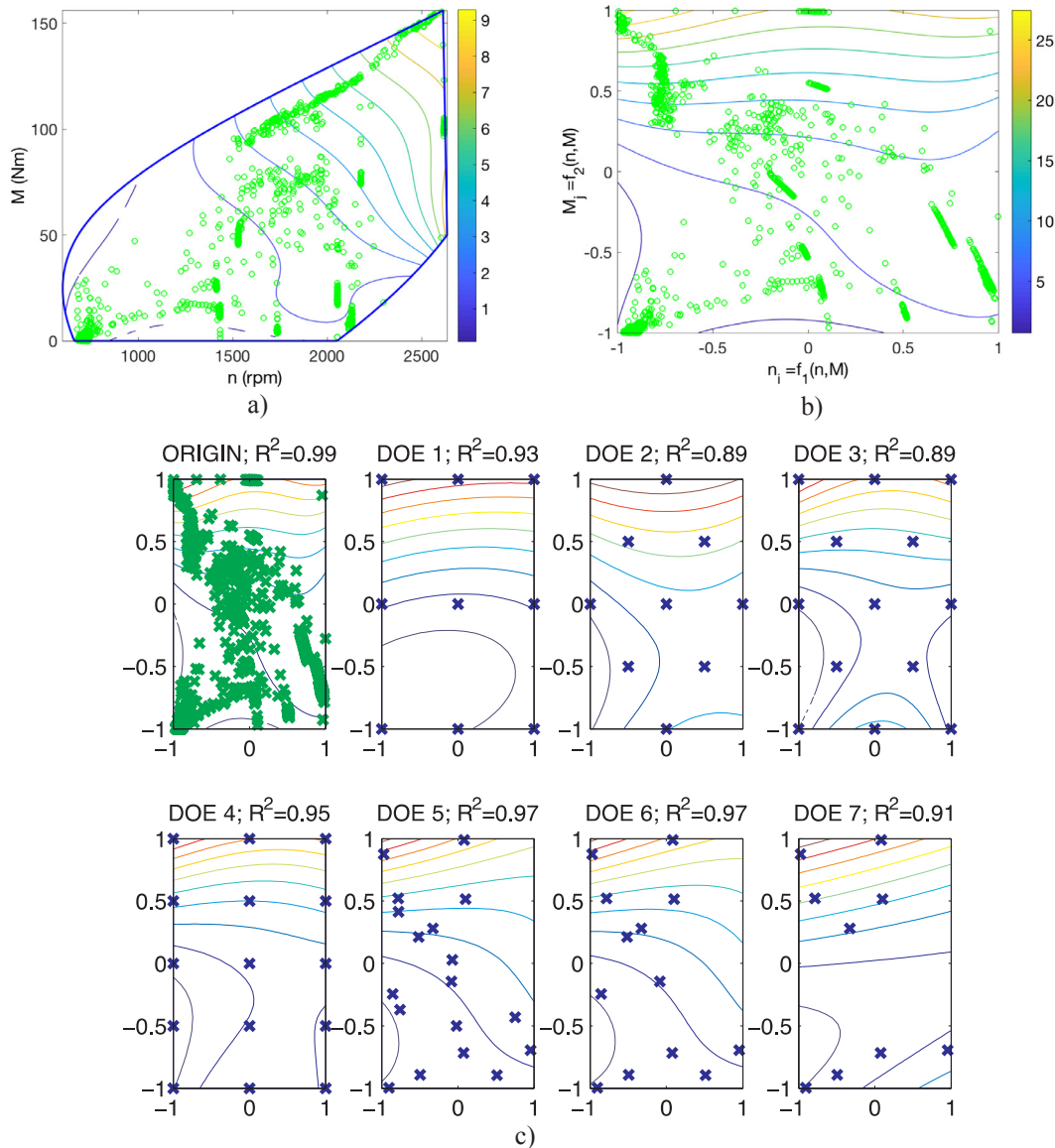


Fig. 14. Contour plots of the exhaust gas residual heat rate response: (a) original surface in the domain n, M (actual engine working space), b) mapping surface in the domain $n_i, M_j \in [-1, 1]$, (c) DoE data including the determination coefficient for each of the seven designs proposed.

3.2. DoE analysis for the responses approximated via a low-degree polynomial

In the present section, the DoE designs proposed in Section 2.6 are applied to those responses selected in Section 3.1. The previously obtained approaches (Section 3.1) are used to generate the synthetic responses for the different points of each DoE. Later, the points of each DoE allow building a new model for each response. Figs. 11–15a and b show the contour plots of these responses in the actual and mapping domains. The new models are used to simulate the NEDC. A comparison between experimental and new estimated instantaneous responses is evaluated through R^2 (see Figs. 11c–15c).

In general, according to the determination coefficients showed in Figs. 11c–15c, all designs give good instantaneous results. Designs 1, 2 and 7 correctly adjust the responses to a second-order polynomial with a minimum of runs, while design 3 and 6 do the same with third-order adjustments. Designs 1 (second order) and 3 (third order) can be applied even by changing the conditions of the test, which means that those designs can be applied to other tests different from NEDC test. However, designs 5, 6 and 7 cannot be generalized, as they characterize

only the current NEDC test. In general, for a specific response, second order designs (DOEs 1, 2 and 7) have less accuracy than third order designs (DOEs 3, 4, 5 and 6).

Next, a DoE analysis for exhaust emissions is included. In order to try to improve exhaust emissions prediction, this DoE study will be based on obtaining, for each analyzed response, a response surface by means of a sum of local models. The flexibility of these local models allows reproducing the high non-linearity of the actual responses surfaces and offers the possibility to improve δ .

According to the determination coefficient, none of the proposed DoE gives enough reliability for instantaneous data (see example in Fig. 16). However, these models provide accurate enough cumulative results for the harmful emissions DoE approaches (see Table 5). For example, DOE 1 and DOE 3 provide a cumulative error lower than 12% and 16% respectively for all exhaust emission responses and satisfy some optimality conditions.

Summarizing, the results show that several DoE with few runs are able to reproduce the following responses: α , VFC , \dot{m}_a , \dot{Q}_{eg} and \dot{E}_{eg} , as well as cumulative harmful emissions. Although the aim of the present study does not include a comparison among the proposed DOEs, basing

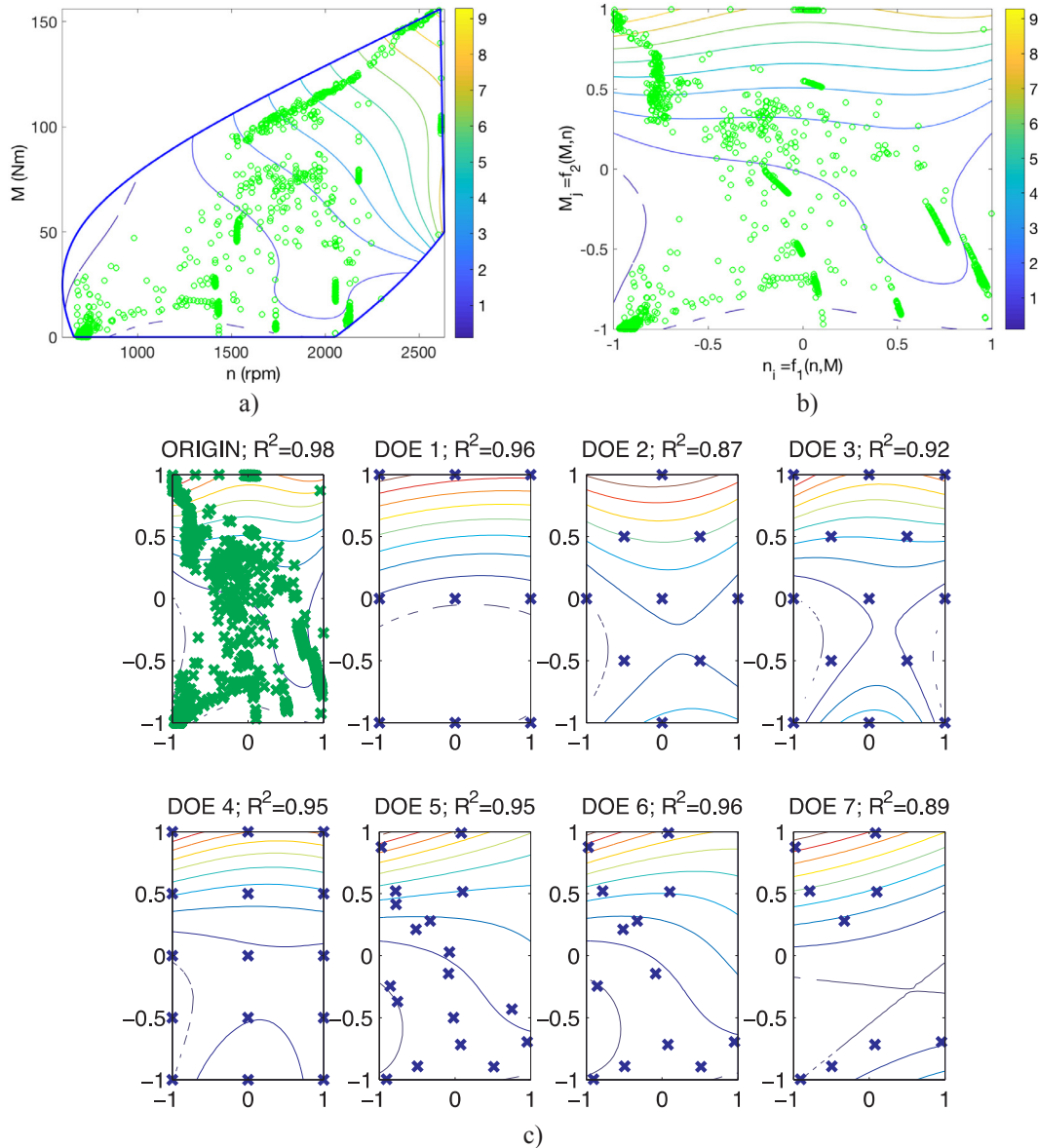


Fig. 15. Contour plots of the exhaust gas thermomechanical exergy rate response: (a) original surface in the domain n, M (actual engine working space), (b) mapping surface in the domain $n_i, M_j \in [-1, 1]$, (c) DoE data including the determination coefficient for each of the seven designs proposed.

on the resulting R^2 and δ , an appropriate design could be the DOE 3, which is an orthogonal array with 13 runs (see Fig. 17) that allows to obtain a third order adjustment. The operating modes showed in Fig. 17a. are obtained by the inverse mapping of the orthogonal array of DOE 3 into the actual engine-working region (see Fig. 17b). For each selected run, the values of n and M factors, which define an operating condition, can be obtained from Fig. 17b.

4. Conclusions

The presented paper studies a methodology to simulate normalized testing cycles for engines and vehicles through design of experiments with low number of runs. The methodology is tested in two stages. The following conclusions can be made from the obtained results:

Regarding the first stage of the methodology (responses fitting):

(a) The following responses can be adjusted, with high accuracy, via smooth surfaces defined by a low-degree polynomial mathematical function: α , VFC , \dot{m}_a , P_{rail} , \dot{Q}_{eg} and \dot{E}_{eg} . The last response is of particular importance because it allows studying the potential of

engine energy recovery.

- (b) Harmful emissions cannot be instantaneously approximated with high accuracy. Nevertheless, the cumulative approximations give satisfactory enough results (low δ) for the following exhaust emission responses: OP , THC , NO_x , CO and CO_2 .
- (c) Rest of responses analyzed can be approximated with enough accuracy by means of more complex functions, such as ANN with multiple factors, but this dependence on multiple factors makes them not appropriate for DoE study with few runs. This is the case of EGR ratio or injection pulse parameters, with the exception of P_{rail} . In any case, the ECU could provide these parameters. For this reason, they are not selected for a DoE analysis.
- (d) Responses that need to be approximated by means of non-smooth surfaces and with a high cumulative error are not suitable for a DoE with few runs.

Regarding the second stage of the methodology (DoE evaluation):

- (a) In order to apply each proposed design, a mapping of the actual engine working region is proposed. This mapping allows testing

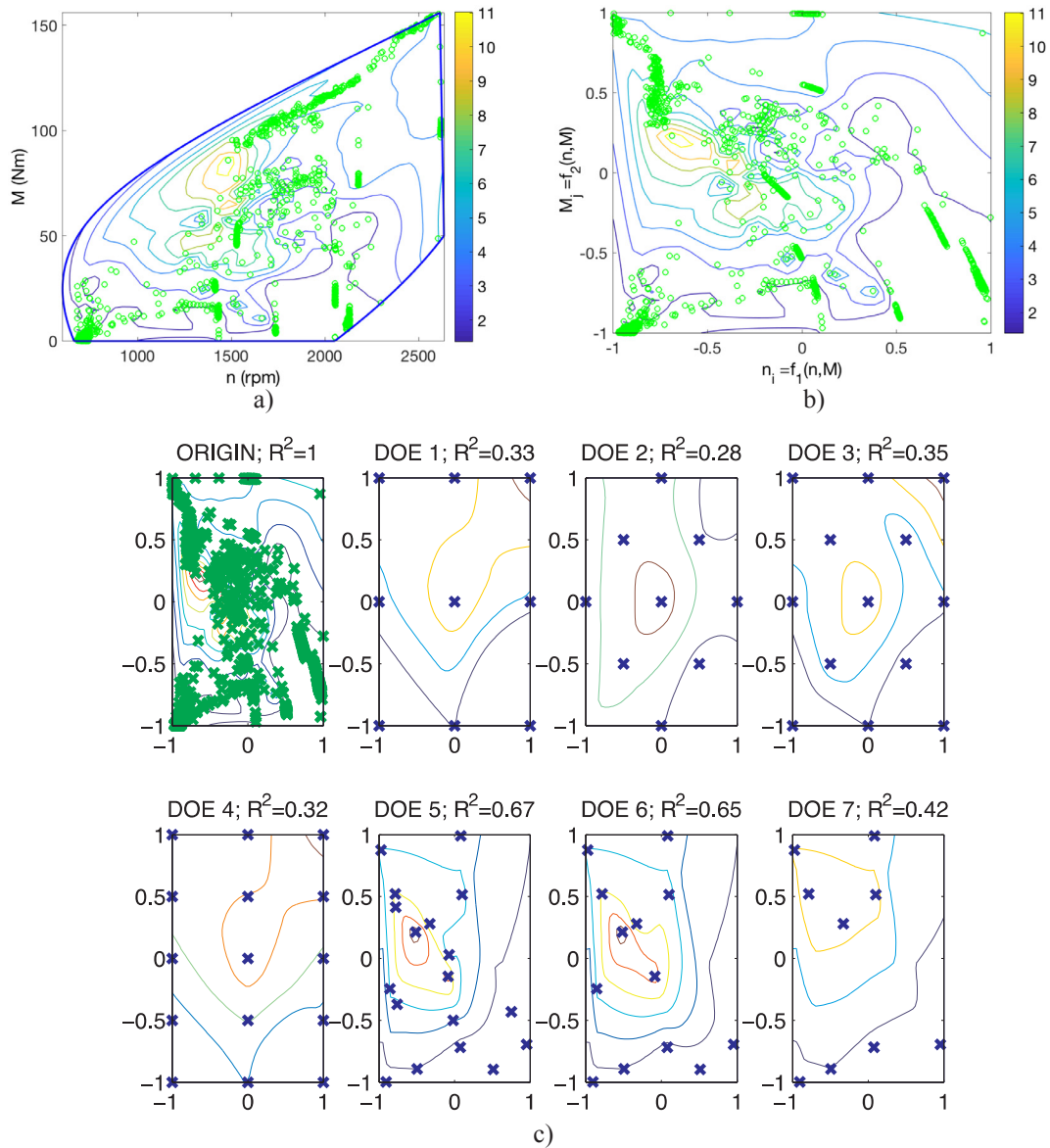


Fig. 16. Contour plots of the opacity response: (a) original surface in the domain n, M (actual engine working space), (b) mapping surface in the domain $n_i, M_j \in [-1, 1]$, (c) DoE data including the determination coefficient for each of the seven designs proposed.

Table 5

Quality of DoE approximations to exhaust emissions responses: cumulative error δ (%).

	DOE 1	DOE 2	DOE 3	DOE 4	DOE 5	DOE 6	DOE 7
<i>OP</i>	9.63	8.10	15.42	5.17	2.99	3.99	14.7
<i>THC</i>	4.54	68.4	11.82	5.16	14.23	24.13	35.1
<i>NO_x</i>	3.11	1.90	0.68	2.11	4.75	5.38	0.58
<i>CO₂</i>	7.67	7.23	4.06	4.96	3.02	3.12	1.96
<i>CO</i>	11.14	56.22	1.58	18.64	16.56	23.15	36.57

each design regardless of the testing cycle, vehicle or engine, because it changes the actual working region into a square domain. In this new working space (mapped region) is easy to apply a DoE that satisfies optimality conditions.

- (b) For those parameters that can be approximated via smooth surfaces, it is demonstrated that all designs give good instantaneous results. Some suitable designs are: DOE 1, which is a full factorial design (9 runs) with a second order adjustment, and DOE 3, which is a fractional factorial design (13 runs) that allows a third order

adjustment.

- (c) Exhaust emissions responses of a test cycle have complex shapes. However, this kind of DoE provides satisfactory cumulative results since the cumulative error is low.

Summarizing, the results show that the proposed methodology demonstrates that it is feasible to replace a whole transient cycle by means of few steady-state operating modes. Several proposed DoEs with few runs allow predicting instantaneous and cumulative engine performance responses via smooth surfaces, as well as cumulative emissions with high accuracy. These findings support the idea of studying the determination of the optimal DoE which minimizes testing time and costs with satisfactory accuracy of engine responses prediction. These future studies will include an improved mapping method, the evaluation of different number of runs (associated to the polynomial approach terms), and the quantification of optimality conditions, as well as the prediction accuracy.

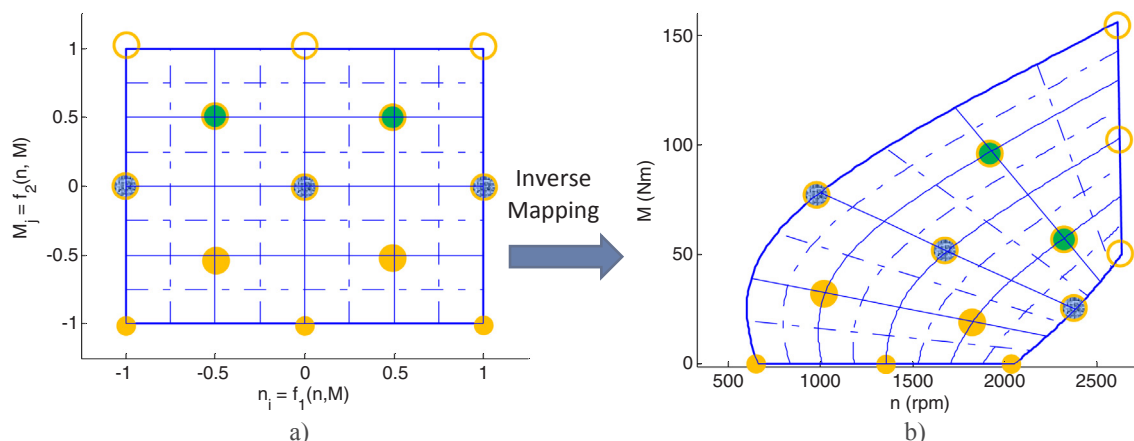


Fig. 17. (a) Design array selected (Design 3–13 runs) in the domain $n_i, M_j \in [-1, 1]$, (b) Selected optimal design into the actual engine-working region.

Acknowledgements

This work was supported by the Spanish Ministry of Economy, Industry and Competitiveness [ENE2014-57043-R]. The authors are also grateful to Repsol Technology Centre laboratories for providing fuel properties.

References

- Ji C, Wang S, Zhang B, Liu X. Emissions performance of a hybrid hydrogen–gasoline engine-powered passenger car under the New European Driving Cycle. *Fuel* 2013;106:873–5.
- Armas O, García-Contreras R, Ramos Á. Pollutant emissions from New European Driving Cycle with ethanol and butanol diesel blends. *Fuel Process Technol* 2014;122:64–71.
- Agudelo AF, García-Contreras R, Agudelo JR, Armas O. Potential for exhaust gas energy recovery in a diesel passenger car under European driving cycle. *Appl Energy* 2016;174:201–12.
- Pacheco AF, Martins ME, Zhao H. New European Drive Cycle (NEDC) simulation of a passenger car with a HCCI engine: emissions and fuel consumption results. *Fuel* 2013;111:733–9.
- Mohamed ES. Development and analysis of a variable position thermostat for smart cooling system of a light duty diesel vehicles and engine emissions assessment during NEDC. *Appl Therm Eng* 2016;99:358–72.
- Nesbit M, Fergusson M, Colsa A, Ohlendorf J, Hayes C, Paquel K, Schweitzer JP. Comparative study on the differences between the EU and US legislation on emissions in the automotive sector, Policy department. Economic and scientific policy. European Parliament. IP/A/EMIS/2016-02, PE 587.331; 2016.
- Tsiakmakis S, Fontaras G, Ciuffo B, Samaras Z. A simulation-based methodology for quantifying European passenger car fleet CO₂ emissions. *Appl Energy* 2017;199:447–65.
- Yang L, Franco V, Mock P, Kolke R, Zhang S, Wu Y, et al. Experimental assessment of NO_x emissions from 73 Euro 6 diesel passenger cars. *Environ Sci Technol* 2015;49:14409–15.
- Giakoumis EG, Zachiotis AT. Investigation of a diesel-engined vehicle's performance and emissions during the WLTC driving cycle—comparison with the NEDC. *Energies* 2017;10:240.
- Pavlovic J, Marotta A, Ciuffo B. CO₂ emissions and energy demands of vehicles tested under the NEDC and the new WLTP type approval test procedures. *Appl Energy* 2016;177:661–70.
- Degrauwe B, Weiss M. Does the New European Driving Cycle (NEDC) really fail to capture the NO_x emissions of diesel cars in Europe? *Environ Pollut* 2017;222:234–41.
- Lapuerta M, Armas O, Rodriguez-Fernandez J. Effect of biodiesel fuels on diesel engine emissions. *Prog Energy Combust Sci* 2008;34:198–223.
- European Parliament and of the council, Regulation (EC) No 715/2007 of the European Parliament and of the council of 20 June 2007 on type approval of motor vehicles with respect to emissions from light passenger and commercial vehicles (Euro 5 and Euro 6) and on access to vehicle repair and maintenance information. *Official Journal of the European Union*; 2007.
- Cárdenas MD, Armas O, Mata C, Soto F. Performance and pollutant emissions from transient operation of a common rail diesel engine fueled with different biodiesel fuels. *Fuel* 2016;185:743–62.
- Gillespie TD. Fundamentals of vehicle dynamics. SAE International; 1992. R-114. ISBN 978-1-56091-199-9 (1999).
- Cárdenas Almendra MD. Estudio de las emisiones de motores diésel de automoción en condiciones de funcionamiento transitorias al usar biodiesel < <http://hdl.handle.net/10578/8793> > ; 2016 [accessed 4 July 2018].
- Castagné M, Bentolila Y, Chaudoye F, Hallé A, Nicolas F, Sinoquet D. Comparison of engine calibration methods based on design of experiments (DoE). *Oil & Gas Sci. Technol.-Revue de l'IFP* 2008;63:563–82.
- Samuel S, Morrey D, Fowkes M, Taylor D, Garner C, Austin L. Numerical investigation of real-world gasoline car drive-cycle fuel economy and emissions. SAE Technical Paper 2004-01-0635; 2004.
- Liu Q, Fu J, Zhu G, Li Q, Liu J, Duan X, et al. Comparative study on thermodynamics, combustion and emissions of turbocharged gasoline direct injection (GDI) engine under NEDC and steady-state conditions. *Energy Convers Manage* 2018;169:111–23.
- García A, Monsalve-Serrano J, Heuser B, Jakob M, Kremer F, Pischinger S. Influence of fuel properties on fundamental spray characteristics and soot emissions using different tailor-made fuels from biomass. *Energy Convers Manage* 2016;108:243–54.
- Belgiorno G, Di Blasio G, Shamun S, Beatrice C, Tunestål P, Tunér M. Performance and emissions of diesel-gasoline-ethanol blends in a light duty compression ignition engine. *Fuel* 2018;217:78–90.
- Cengel YA, Boles MA. Thermodynamics: an engineering approach. Sea 2002;1000:8862.
- Edwards AWF. Pascal's Arithmetical Triangle: The Story of a Mathematical Idea. Baltimore and London: JHU Press; 2002.
- Wu CFJ, Hamada MS. Experiments: planning, analysis, and optimization. 2 ed. John Wiley & Sons; 2011.
- Khuri AI, Mukhopadhyay S. Response surface methodology. *Wiley Interdiscip Rev Comput Stat* 2010;2:128–49.
- Baker FD, Bargmann RE. Orthogonal central composite designs of the third order in the evaluation of sensitivity and plant growth simulation models. *J Am Stat Assoc* 1985;80:574–9.
- Li H, Butts K, Zaseck K, Liao-McPherson D, Kolmanovsky I. Emissions modeling of a light-duty diesel engine for model-based control design using multi-layer perceptron neural networks. SAE Technical Paper 2017-01-0601; 2017.
- Abramowitz M, Stegun IA. Handbook of mathematical functions: with formulas, graphs, and mathematical tables. Courier Corporation 1964.
- Cruz-Peragon F, Jimenez-Espadafor FJ, Palomar JM, Dorado MP. Combustion faults diagnosis in internal combustion engines using angular speed measurements and artificial neural networks. *Energy Fuels* 2008;22:2972–80.
- Yusaf TF, Buttsworth D, Saleh KH, Yousef B. CNG-diesel engine performance and exhaust emission analysis with the aid of artificial neural network. *Appl Energy* 2010;87:1661–9.
- Cruz-Peragón F, Jiménez-Espadafor FJ. Design and optimization of neural networks to estimate the chamber pressure in internal combustion engines by an indirect method. *Energy Fuels* 2007;21:2627–36.
- Yang F, Cho H, Zhang H, Zhang J, Wu Y. Artificial neural network (ANN) based prediction and optimization of an organic Rankine cycle (ORC) for diesel engine waste heat recovery. *Energy Convers Manage* 2018;164:15–26.
- Fausett L, Fausett L. Fundamentals of neural networks: architectures, algorithms, and applications. Prentice-Hall; 1994.
- MacKay DJ. Bayesian nonlinear modeling for the prediction competition. *ASHRAE Trans* 1994;100:1053–62.
- Casanova-Peláez PJ, Palomar-Carnicero JM, Manzano-Agugliaro F, Cruz-Peragón F. Olive cake improvement for bioenergy: the drying kinetics. *Int J Green Energy* 2015;12:559–69.
- Joumard R, Andre J, Rapone M, Zallinger M, Kljun N, Andre M, et al. Emission factor modelling and database for light vehicles-Artemis deliverable 3 (2007) Annex 12, pp. 143.
- Yusri I, Mamat R, Azmi W, Omar A, Obed M, Shaiful A. Application of response surface methodology in optimization of performance and exhaust emissions of secondary butyl alcohol-gasoline blends in SI engine. *Energy Convers Manage* 2017;133:178–95.
- Franco V, Kousolidou M, Muntean M, Ntziachristos L, Hausberger S, Dilara P. Road vehicle emission factors development: a review. *Atmos Environ* 2013;70:84–97.
- Velmurugan DV, Grahn M, McKelvey T. Diesel engine emission model transient cycle validation. *IFAC-PapersOnLine* 2016;49:1–7.
- Weilenmann M, Favez J, Alvarez R. Cold-start emissions of modern passenger cars at different low ambient temperatures and their evolution over vehicle legislation categories. *Atmos Environ* 2009;43:2419–29.